1984

On formation of coastal deserts

Kuo, H.L.; Chu, Peter C.

Kuo, H.L., and P.C. Chu, 1984: On formation of coastal deserts. Third Conference on Meteorology of the Coastal Zone, American Meteorological Society, 17-22
http://hdl.handle.net/10945/36219

2.5

ON FORMATION OF COASTAL DESERTS

H.L. Kuo and P.C. Chu
The University of Chicago
Chicago, IL 60637

1. INTRODUCTION

Observations indicate that almost all the desert areas along the coasts of various continents in the subtropics have high and steep mountains and are associated with equatorward longshore winds and oceanic coastal upwellings. The most prominent example is the Chilean-Peruvian coastal desert which is associated with the longest stretch of longshore wind (see Lydolph, 1973). It is the opinion of the senior author that these longshore winds are the products of the blocking effect of the coastal mountain chains on the mean winds normal to it, and the primary meteorological cause of desert generation is the descending motion associated with this equatorward longshore wind, partly from the divergence field of this wind itself while another part is from the secondary flow in the vertical plane normal to the coast produced by the frictional force and differential heating from the coastal upwelling effect. In this paper we shall at first use the linearized vorticity equation with eddy dissipation to demonstrate this blocking effect on longshore wind generation, and then use the linear surface boundary layer equations to obtain the secondary flow. For simplicity, we take the coast as oriented in NS direction, but the results can also be applied to a slantly oriented coast by using the mean wind in the normal direction only.

2. LONGSHORE WIND GENERATION BY MOUNTAIN-BLOCKING IN SUBTROPICAL HIGH PRESSURE REGION

We consider the undisturbed flow in the subtropical high pressure region far away from the mountain-chain along the coast of the continent as purely zonal and denote it by U(y), and take the perturbation created by the blocking effect of the mountain-chain as represented by the linearized steady state barotropic vorticity equation with dissipation which we shall write in terms of the stream function Ψ' as

$$\nu\nabla^4\Psi' - U\frac{\partial\nabla^2\Psi'}{\partial x} - \beta\frac{\partial\Psi'}{\partial x} = 0, \tag{1}$$

where ν is the large-scale horizontal eddy mixing coefficient, $\beta = df/dy$ is the Rossby parameter and $\nabla^2 = \partial^2/\partial x^2 + \partial^2/\partial y^2$.

In general, the zonal current U is westerly on the higher latitude side and easterly on the equator side of the subtropical high pressure belt, and it can be represented by the expression

$$U = U(\eta) = \bar{U} + U_1 \sin\eta + \hat{U}_1 \cos\eta + U_2 \sin 2\eta + \hat{U}_2 \cos 2\eta + \ldots, \tag{2}$$

where $\eta = \pi(y - y_o)/2L$, y_o is the distance from the high center to equator and L is the distance between the centers of the westerly branch and the easterly branch. The stream function Ψ_I defined by the relation $d\Psi_I/d\eta = -2LU/\pi$ is given by

$$\Psi_I(\eta) = \Psi_{Io} - \frac{2L}{\pi}\{U_1 + 1/2U_2 + \bar{U}\eta + \hat{U}_1 \sin\eta - U_1\cos\eta + 1/2\,\hat{U}_2 \sin 2\eta - 1/2U_2\cos 2\eta + \ldots\} = \tilde{\Psi}_{Io} + \Psi_{I1}\sin\eta + \hat{\Psi}_{I1}\cos\eta + \Psi_{I2}\sin 2\eta + \hat{\Psi}_{I2}\cos 2\eta + \ldots \tag{3}$$

If we take the range of η as from $-\pi$ to π, we then have

$$\eta = 2(\sin\eta - 1/2\sin 2\eta + 1/3\sin 3\eta - \ldots) \quad (-\pi<\eta<\pi) \tag{3a}$$

and therefore

$$\tilde{\Psi}_{Io} = \Psi_{Io} - \frac{2L}{\pi}(U_1 + 1/2U_2),\ \Psi_{I1} = -\frac{2L}{\pi}(2\bar{U} + \hat{U}_1),$$
$$\hat{\Psi}_{I1} = \frac{2L}{\pi}U_1,\ \Psi_{I2} = \frac{2L}{\pi}(\bar{U} - 1/2\hat{U}_2),$$
$$\hat{\Psi}_{I2} = \frac{L}{\pi}U_2. \tag{3b-f}$$

On the other hand, if we take the range of η as from $-\pi/2$ to $\pi/2$, inclusive, we then have

$$\eta = \frac{4}{\pi}(\sin\eta - \frac{1}{9}\sin 3\eta + \frac{1}{25}\sin 5\eta - \ldots), \tag{3a*}$$

and

$$\tilde{\Psi}_{Io} = \Psi_{Io} - \frac{2L}{\pi}(U_1 + 1/2U_2),\ \Psi_{I1} = \frac{-2L}{\pi}\hat{U}_1 - \frac{8L}{\pi^2}\bar{U},$$
$$\hat{\Psi}_{I1} = \frac{2L}{\pi}U_1,\ \Psi_{I2} = -\frac{L}{\pi}\hat{U}_2,\ \hat{\Psi}_{I2} = \frac{L}{\pi}U_2. \tag{3b*-f*}$$

Since Ψ_{Io} is arbitrary, we shall set it to $2LU_1/\pi$ so that we have

$$\tilde{\Psi}_{Io} = -\frac{LU_2}{\pi} = -\hat{\Psi}_{I2}. \tag{3a*}$$

we write the solution of (1) in the following form

$$\Psi'(x,y) = \Psi_o(x) + \hat{\Psi}_1(x)\sin\eta + \Psi_1(x)\cos\eta + \Psi_2(x)\sin 2\eta + \hat{\Psi}_2(x)\cos 2\eta + \ldots \tag{4}$$

Substituting (4) in (1) we then find the following set of equations:

$$\nu d^4\Psi_o - \bar{U}d^3\Psi_o - \beta d\Psi_o = \frac{U_1}{2}(d^3\Psi_1 - \mu^2 d\Psi_1), \tag{5}$$

$$\nu(d^2 - \mu^2)^2\Psi_1 - \bar{U}(d^3\Psi_1 - \mu^2 d\Psi_1) - \beta d\Psi_1 = U_1[D^3\Psi_o - 1/2(d^3\hat{\Psi}_2 - 4\mu^2 d\hat{\Psi}_2)], \tag{6}$$

$$\nu(d^2 - \mu^2)^2\hat{\psi}_1 - \bar{U}(d^3\hat{\psi}_1 - \mu^2 d\hat{\psi}_1) - \beta d\hat{\psi}_1 = \frac{U_1}{2}(D^3\psi_2 - 4\mu^2 d\psi_2), \quad (7)$$

$$\nu(d^2 - \mu^2)^2\psi_2 - \bar{U}(d^3\psi_2 - 4\mu^2 d\psi_2) - \beta d\psi_2 = \frac{U_1}{2}(d^3\hat{\psi}_1 - \mu^2 d\hat{\psi}_1), \quad (8)$$

$$\nu(d^2 - \mu^2)^2\hat{\psi}_2 - \bar{U}(d^3\hat{\psi}_2 - 4\mu^2 d\hat{\psi}_2) - \beta d\hat{\psi}_2 = -\frac{U_1}{2}(d^3\psi_1 - \mu^2 d\psi_1) \quad (9)$$

where $d = d/\partial x$ and $\mu = \pi/2L$. These equations show that the width of the lateral boundary is of the order of the Munk boundary layer width δ defined by

$$\delta = (\nu/\beta)^{1/3} \quad (10)$$

Here we take ν as of the order of $10^5 m^2 s^{-1}$ for the large-scale flow, and β equal to $2 \times 10^{-11} m^{-1} s^{-1}$. We then find that δ is about 170 km. Since L is of the order 2×10^3 km, we have $\mu^2\delta^2 << 1$. Therefore all the μ^2 terms in the above equations can be neglected so that they reduce to the following in terms of $\xi = x/\delta$:

$$(D^3 - aD^2 - 1)\psi_o = -a_o D^2\psi_1, \quad (11)$$

$$(D^3 - aD^2 - 1)\psi_1 = -2a_o D^2(\psi_o - \tfrac{1}{2}\hat{\psi}_2), \quad (12)$$

$$(D^3 - aD^2 - 1)\hat{\psi}_1 = -a_o D^2\psi_2, \quad (13)$$

$$(D^3 - aD^2 - 1)\psi_2 = -a_o D^2\hat{\psi}_1, \quad (14)$$

$$(D^3 - aD^2 - 1)\hat{\psi}_2 = a_o D^2\psi_1 \quad (15)$$

where

$$D = \frac{d}{d\xi}, \quad a = \frac{\bar{U}}{\beta\delta^2}, \quad a_o = -\frac{U_1}{2\beta\delta^2}. \quad (16)$$

From (13) and (14) we find that ψ_1 and ψ_2 satisfy the following equation

$$[D^3 - (a + a_o)D^2 - 1] \cdot [D^3 + (a_o - a)D^2 - 1](\hat{\psi}_1, \psi_2) = 0. \quad (17)$$

We take (11) minus (15)/2 and write the resulting equation and (12) in terms of $\phi = \psi_o - 0.5\hat{\psi}_2$ as

$$(D^3 - aD^2 - 1)\phi = -\frac{3a_o}{2}D^2\psi_1, \quad (18)$$

$$(D^3 - aD^2 - 1)\psi_1 = -2a_o D^2\phi, \quad (19)$$

From these equations we find that ψ_1 and ϕ satisfy the following equation:

$$[D^3 - (\sqrt{3}a_o + a)D^2 - 1] \times [D^3 + (\sqrt{3}a_o - a)D^2 - 1](\psi_1, \phi) = 0 \quad (20)$$

On taking the sum of (11) and (15) we find that the function $\phi^* = \psi_o + \hat{\psi}_2$ satisfies

$$(D^3 - aD^2 - 1)\phi^* = 0. \quad (21)$$

The general solutions of the equations (17) and (20) can be written as

$$\hat{\psi}_1 = \sum_{j=1}^{3} (\hat{\psi}_{1j}e^{\alpha_j\xi} + \hat{\psi}'_{1j}e^{\alpha'_j\xi}) \quad (22)$$

$$\psi_1 = \sum_{j=1}^{3} (\psi_{1j}e^{\gamma_j\xi} + \psi'_{1j}e^{\gamma'_j\xi}), \quad (23)$$

where α_j, α'_j, γ_j, γ'_j, are the roots of the following cubic equations:

$$\alpha^3 - (a_o + a)\alpha^2 - 1 = 0, \quad (24a)$$

$$\alpha'^3 - (a - a_o)\alpha'^2 - 1 = 0, \quad (24b)$$

$$\gamma^3 - (\sqrt{3}a_o + a)\gamma^2 - 1 = 0, \quad (25a)$$

$$\gamma'^3 - (a - \sqrt{3}a_o)\gamma'^2 - 1 = 0 \quad (25b)$$

Observe that the change of the sign of a_o, such as from the zonal velocity profile of southern hemisphere to that of the northern hemisphere merely interchanges α with α' and γ with γ'.

For the normal values $\bar{U} = 2ms^{-1}$, $U_1 = -8ms^{-1}$, $\beta = 2 \times 10^{-11} m^{-1}s^{-1}$, $\nu = 1 \times 10^5 m^2 s^{-1}$ we then have $a = 3.42$, $a_o = 6.84$ and

$$\alpha_1 = 10.26965, \quad \alpha_{2,3} = -0.002483 \pm 0.31036i,$$

$$\alpha'_1 = 0.50487, \quad \alpha'_2 = 0.5950, \quad \alpha_3 = -3.3300;$$

$$\gamma_1 = 15.27186, \quad \gamma_{2,3} = -.0020115 \pm 0.058066i,$$

$$\gamma'_1 = 0.33700, \quad \gamma'_2 = -0.35141, \quad \gamma'_3 = -8.41309 \quad (26)$$

Since the perturbation stream function is required to vanish at a great distance from $\xi = 0$, we can only use the exponentially decaying terms in (22) and (23). In addition, the solution must also satisfy the kinematic and dynamic conditions along the mountain barrier. For convenience we place the origin of ξ at the longitude of the NS-oriented mountain chain. Since the stream line must coincide with the barrier, we can set the total stream function $\psi_I + \psi'$ to zero there, so that at $\xi = 0$ we have

$$\psi_o = -\bar{\psi}_{Io}, \quad \psi_1 = -\psi_{I1}, \quad \hat{\psi}_1 = -\hat{\psi}_{I1}, \text{ etc.} \quad (27a)$$

In addition, we assume the geophysical condition that the tangential stress on the mountain is parallel to the wind, so that we have

$$v = K\frac{dv}{d\xi} \quad (27b)$$

where K is a proportionality factor defined by

$$|K| = \frac{\rho\nu v(o)}{\delta t_b}$$

where δ is given by (10) and t_b is the tangential stress on the boundary. Here $K = 0$ represents no slip and $|K| = \infty$ represents zero stress, and the

sign of K is the same as that of ξ.

From (21) we find that these conditions cannot be satisfied simultaneously by the solution of this equation except when Φ' is identically zero. Therefore we set

$$\hat{\Psi}_2 = -\Psi_o, \quad \Phi = \Psi_o - \frac{1}{2}\hat{\Psi}_2 = \frac{3}{2}\Psi_o,$$

so that all the functions Ψ_o, Ψ_1 and $\hat{\Psi}_2$ satisfy (20).

2a. SOLUTION FOR AN EASTERN BOUNDARY

For the region with the mountain on the east side such as near the west coasts of North and South America, Africa and Australia, we can only use solutions with positive real exponents, so that we have,

$$\hat{\Psi}_1 = \hat{\Psi}_{11} e^{\alpha_1 \xi} + \hat{\Psi}'_{11} e^{\alpha'_1 \xi}, \tag{28}$$

$$\Psi_1 = \Psi_{11} e^{\gamma_1 \xi} + \Psi'_{11} e^{\gamma'_1 \xi}. \tag{29}$$

The no-slip condition is satisfied provided we have

$$\hat{\Psi}_{11} = \frac{\alpha'_1}{\alpha_1 - \alpha'_1}\hat{\Psi}_{1I}, \qquad \hat{\Psi}'_{11} = -\frac{\alpha_1}{\alpha'_1}\hat{\Psi}_{11};$$

$$\Psi_{11} = \frac{\gamma}{\gamma\ \ \gamma}\Psi_{1I}, \qquad \Psi'_{11} = -\frac{\gamma_1}{\gamma'_1}\Psi_{11}. \tag{30a-d}$$

Thus for the zonal velocity profile whose coefficients U_1, U_2 and U_2 are small, such as shown in Fig. 1, the total stream function Ψ and the longshore velocity v are approximately given by

$$\Psi(\xi,\eta) = \Psi_{1I}\{1 + \frac{1}{(\gamma - \gamma')}[\gamma'_1 e^{\gamma_1 \xi} - \gamma_1 e^{\gamma'_1 \xi}]\} \sin\eta + \hat{\Psi}_{1I}\{1 + \frac{1}{\alpha_1 - \alpha'_1}[\alpha'_1 e^{\alpha_1 \xi} - \alpha_1 e^{\alpha'_1 \xi}]\} \cos\eta, \tag{31}$$

$$v = \frac{\gamma_1 \gamma'_1}{\delta(\gamma_1 - \gamma'_1)}(e^{\gamma_1 \xi} - e^{\gamma'_1 \xi})\Psi_{1I} \sin\eta + \frac{\alpha_1 \alpha'_1}{\delta(\alpha_1 - \alpha'_1)}(e^{\alpha_1 \xi} - e^{\alpha'_1 \xi})\hat{\Psi}_{1I} \cos\eta. \tag{32}$$

This solution gives an equatorward longshore jet close to the coast, as illustrated in Fig. 2, where the upward coordinate is toward the equator and the middle point corresponds to the mid-point of the subtropical high pressure belt, with L taken as equal to 2000 km. We mention that the mid-point of the high pressure belt usually inclines upward toward the equator. It is seen that as the westerly current approaches the mountain-chain it turns equatorward and creates a strong longshore jet with its maximum velocity reaching 15 ms^{-1}, almost double the maximum undisturbed zonal wind speed.

From (32) and the values of α_1, α'_1, γ_1, γ'_1 given above we find that the maximum of the longshore jet occurs at a distance about 0.278 times the boundary thickness δ given by (10), which is about 47 km. This is very close to the distances from the center of the observed longshore jet off the Oregon coast to the coastal mountain chain (see Elliot and O'Brien, 1977). The variations of the longshore wind with ξ at different latitude across the belt are illustrated in Fig. 3. These results show that the width of the longshore jet produced by the blocking effect of the mountain is of the order of 100 km. However, we can only consider this value as of the right order of magnitude on account of the uncertainty of the value of ν. On the other hand, it seems that the geostrophic stress relation with a finite K would give a better representation of observed velocity variations close to the mountain barrier than the no slip condition, we shall therefore derive the solution near the eastern boundary under this stress condition in the next sub-section.

2b. SOLUTION NEAR THE EASTERN BOUNDARY WHICH SATISFIES THE GEOSTROPHIC STRESS CONDITION WITH FINITE COEFFICIENT.

Since the domain under consideration is $-\infty<\xi<0$, the factor K must be taken as negative, so that we have $-K = K^*>0$. It can readily be shown that the solution of Eq. (1) which satisfies the conditions (27a) and (27b) for the eastern boundary is given by

$$\Psi = \{1 + \frac{1}{(\gamma_1 - \gamma'_1)[1+K'(\gamma_1+\gamma'_1)]}[\gamma'_1(1 + K^*\gamma'_1)e^{\gamma_1 \xi} - \gamma_1(1 + K^*\gamma_1)e^{\gamma'_1 \xi}]\}\Psi_{1I} \sin\eta + \{1 + \frac{1}{(\alpha_1 - \alpha'_1)[1+K^*(\alpha_1+\alpha'_1)]}[\alpha'_1(1 + K^*\alpha'_1)e^{\alpha_1 \xi} - \alpha_1(1+K^*\alpha_1)e^{\alpha'_1 \xi}]\}\hat{\Psi}_{1I} \cos\eta. \tag{33}$$

From this solution we find that for a finite K*, the gradient of v and the distance from the jet center to the boundary are smaller than that given by the no slip condition.

2c. SOLUTION FOR A WESTERN BOUNDARY

When the mountain barrier is on the western end of the region such as that along the East coast of Africa, only the negative real roots α'_2 α'_3 γ'_2 and γ'_3 in (26) can be used in the solutions (22) and (23) so that for the no-slip condition we have

$$\Psi = \{1 + \frac{1}{\gamma'_2 - \gamma'_3}(e^{\gamma'_2 \xi} - e^{\gamma'_3 \xi})\}\Psi_{1I} \sin\eta + \{1 + \frac{1}{\alpha'_2 - \alpha'_3}(e^{\alpha'_2 \xi} - e^{\alpha'_3 \xi})\}\hat{\Psi}_{1I} \cos\eta. \tag{34}$$

From the values given in (26), we find that α'_2/α'_3 and γ'_2/γ'_3 are larger than α'_1/α_1 and γ'_1/γ_1 and the differences $\alpha'_2-\alpha'_3$ and $\gamma'_2-\gamma'_3$ and and the absolute values of α'_3, γ'_3 are smaller than $\alpha_1-\alpha'_1$, $\gamma_1-\gamma'_1$, α_1 and γ_1. Therefore the western boundary layer is wider and the center of the longshore jet is at a larger distance from the boundary than that in the eastern boundary layer for the same zonal velocity.

The solution which satisfies the slip geostrophic stress condition for this case is given by an expression similar to (33), with α_1, α_1', γ_1, γ_1' and K* replaced by α_2', α_3', γ_2', γ_3' and K.

2d. THE DIVERGENCE FIELD OF LONGSHORE WIND

Since the boundary layer flow is of large scale and steady, the Coriolis force associated with it must be balanced by a cross wind pressure gradient so that we have the geostrophic relation

$$u_g = -\frac{1}{f}\frac{\partial \phi}{\partial y}, \quad v_g = \frac{1}{f}\frac{\partial \phi}{\partial x}, \tag{35}$$

where ϕ is the geopotential of the isobaric surface and is equal to the Coriolis parameter f times the stream function Ψ. Since f varies with latitude, this longshore wind possesses a divergence and hence is also accompanied by a vertical velocity w_g which are given by the following expressions:

$$\nabla . V_g = -\frac{\beta}{f} v_g. \tag{36}$$

$$w_g(z) = \frac{\beta}{f} v_g z. \tag{37}$$

Thus, with a mean equatorward velocity of 7.5 ms^{-1} extending from the surface to the 3 km level at 20°, (37) gives a downward velocity of 0.90 cm s^{-1}, which is fairly large and is of primary importance for the climate of the region.

In addition, this equatorward longshore wind also produces an upwelling of cold water in the ocean along the coast and hence an ocean surface temperature anomaly. The influences of the differential heating resulting from this surface temperature anomaly and that of the frictional force on the secondary flow will be investigated in the next section.

3. EFFECTS OF DIFFERENTIAL HEATING AND FRICTION ON SECONDARY CIRCULATION

We take the longshore wind v_g, the accompanying vertical velocity w_g and the ocean surface temperature difference ΔT_w produced by upwelling as given and investigate the disturbances generated by the related frictional and thermal forces in the vertical plane normal to the coast. The perturbation is considered as hydrostatic and steady and independent of the longshore coordinate y, and dissipation is in vertical directly only with both the eddy viscosity coefficient and the eddy diffusion coefficient given by ν_e. For convenience, we measure the coast-normal coordinate x in unit of horizontal scale L (~200 km ~δ), the vertical coordinate z in unit of the Ekman depth $\delta_e = (\nu e/2\Omega)^{1/2}$ where Ω is the angular velocity of earth rotation, the horizontal velocities in unit of the velocity scale U, vertical velocity in $U\delta_e/L$, pressure in unit of $2\Omega\rho_o LU$ and set the potential temperature perturbation θ' to $2\Omega LU\theta_o s/g\delta_e$. We then find that the linearized equation of motion, heat equation and continuation equation are given in dimensionless forms by

$$D^2 u + \eta v = P_x \tag{38}$$

$$D^2 v - \eta u = 0 \tag{39}$$

$$P_z = s \tag{40}$$

$$D^2 s - R_i w = 0 \tag{41}$$

$$u_x + w_z = 0 \tag{42}$$

where

$$D = d/dz, \quad R_i = \frac{g}{4\Omega^2 L^2}\frac{1}{\theta_o}\frac{\partial \theta_o}{\partial z}\delta_e^2, \eta = \sin\Phi \tag{43}$$

The change of the potential temperature produced by the vertical velocity w_g can be obtained directly from (41) and is given by

$$\hat{\theta} = \frac{\beta}{12\Omega\nu_e\eta}\frac{\partial \theta_o}{\partial z} v_g(x) z'(z'^2 - h^2) \quad 0 \leqslant z' \leqslant h.$$

where h is the depth of the longshore wind. Here it is assumed that v_g remains constant below h and the perturbation vanishes above h. Since w_g is from $\partial vg/\partial y$, there is no u velocity associated with it.

Eq (42) indicates that the velocities u and w can be represented by the stream function Ψ, viz,

$$u = -D\Psi, \quad w = \Psi_x. \tag{44}$$

Eliminating v, p and s from (38)-(41) we then find that Ψ is given by the following equation

$$(D^4 + \eta^2)D^2\Psi + R_i\Psi_{xx} = 0. \tag{45}$$

These equations are the same as those derived by Kuo (1973) in his treatment of the planetary boundary and they will also be solved in a similar manner, namely, by expanding Ψ, v and s in Fourier series in x-direction, viz.,

$$\Psi(x,z) = \sum_{n=1}^{\infty} \Psi_n(z) \sin n\pi x,$$

$$v(x,z) = \sum_{n=1}^{\infty} v_n(z) \sin n\pi x,$$

$$s(x,z) = \sum_{n=0}^{\infty} s_n(z) \cos n\pi x. \tag{46a,b,c}$$

Here an infinity series is required on account of the variations of v_g and the ocean surface temperature with x. Substituting these expansions in (45), (39) and (41) and equating the coefficients of the individual Fourier components to zero we then obtain the following set of equations

$$D^6\Psi_n + \eta^2 D^2\Psi_n - n^2\pi^2\Psi_n = 0, \tag{47}$$

$$D^2 v_n = -\eta D\Psi_n, \tag{48}$$

$$D^2 s_n = n\pi R_i \Psi_n. \tag{49}$$

The boundary conditions we impose on these functions are

Ψ_n, v_n, s_n remain finite as $\zeta \to \infty$ (50a)

$\Psi_n = D\Psi_n = 0$, $v_n = -v_{gn}$, $s_n = s_{no}$ for $\zeta=0$ (50b)

The solution of Eq (47) which satisfy these conditions for Ψ_n and $D\Psi_n$ is given by

$$\Psi_n(\zeta) = C_n\{e^{\lambda_1\zeta} + \frac{\lambda_1-\lambda_3}{\lambda_3-\lambda_2}e^{\lambda_2\zeta} + \frac{\lambda_2-\lambda_1}{\lambda_3-\lambda_2}e^{\lambda_3\zeta}\}. \quad (51)$$

where λ_1, λ_2 and λ_3 are the three roots of the auxiliary equation of (47) with negative real parts and C_n is arbitrary constant. Using this Ψ_n in (48) and (49) we find the corresponding functions v_n and s_n are given by

$$v_n = D_n - \eta C_n\{\frac{1}{\lambda_1}e^{\lambda_1\zeta} + \frac{1}{\lambda_3-\lambda_2}[\frac{\lambda_1-\lambda_3}{\lambda_2}e^{\lambda_2\zeta} + \frac{\lambda_2-\lambda_1}{\lambda_3}e^{\lambda_3\zeta}]\} \quad (52)$$

$$s_n = n\pi R_i\{\frac{1}{\lambda_1^2}e^{\lambda_1\zeta} + \frac{1}{\lambda_3-\lambda_2}[\frac{\lambda_1-\lambda_3}{\lambda_2^2}e^{\lambda_2\zeta} + \frac{\lambda_2-\lambda_1}{\lambda_3^2}e^{\lambda_3\zeta}]\} \quad (53)$$

where D_n and C_n are determined by the conditions for v and s at the surface.

For simplicity we take v_g as given by

$$v_g = -v_{go}e^{\alpha\xi}\sin\pi\xi \quad (54)$$

with $\alpha = 0.34657$ and $v_{go} = 9.5$ ms^{-1}, and an ocean surface temperature difference ΔT_w resulting from upwelling equal to 5°C. The ocean surface temperature is taken as equal to $T_o - T_w$ in the 40 km wide strip along the coast and equal to T_o farther away. The mountain is located 40 km from the coast inland. Notice that the longshore wind v_g possess positive vorticity on the land side and negative vorticity on the ocean side

Solutions of the equations (47)-(49) have been obtained for three different cases, namely,

i) with all the driving forces mentioned above present,

ii) with ΔT_w present but with the longshore wind effect absent,

iii) with the longshore wind v_g and the associated w_g but with $\Delta T_w = 0$.

The stream function Ψ and the total vector velocity $ui + (w + w_g)k$ obtained for case iii) are represented in Figs. 4a and 4b, respectively. These results are almost indistinguishable from those in case i) where both the mechanical and the thermal driving forces are present, showing the dominance of the vertical motion by the Ekman suction and w_g associated with the longshore wind. From Fig. 4b we see that descending motion prevails at high levels for all x, and also in the coastal strip and farther away at low levels. The maximum descending motion for this case is about 1 cm s^{-1} and the maximum upward velocity is about 0.4 cm s^{-1} and it occurs at low levels close to the mountain. Fig. 4b shows that the circulation produced by the thermal effect of ocean surface temperature difference ΔT_w in the coastal region is a two-cell type circulation with stronger descending motion occurring in a narrow coastal strip, and upward motion away from the coast. As is shown in another paper, the circulation is greatly intensified during day time on account of the diurnal variation of solar radiation, but the general pattern is not altered significantly.

4. CONCLUDING REMARKS

It has been shown by our analysis that the blocking effect of the coastal mountain chain on the mean zonal flow in the subtropics creates a strong equatorward longshore wind, and the frictional drag on this longshore wind and the ocean surface temperature anomaly created by the upwelling caused by the surface drag produce a secondary circulation with intense descending motion in a relatively narrow strip close to and over some distance from the coast inland. Further, the geostrophic equatorward longshore wind is also associated with a descending velocity, which makes the whole region dominated by descending motion above the surface boundary layer. The combination of these flows makes these coastal regions arid, especially in the coastal strip where downward motion prevails at all levels.

References

Elliot, J.S., and J.J. O'Brien, 1977: Observational studies of the marine boundary layer over an upwelling region. Mon. Wea. Rev., 105, 86-98.

Kuo, H.L., 1973: Planetary boundary layer flow of a stable atmosphere over the globe. J. Atmos. Sci., 30, 53-65

Lydolph, P.E., 1957: A comparative analysis of the dry western littorals. Asso. Amer. Geographers' Annuals, 47(3), 213-230.

Moody, G.L., David W. Stuart, A.I. Watson and M.M. Nanny, 1981: Sea-surface temperatures and winds during JOINT II, part 1, mean conditions. In: Coastal Upwelling. Amer. Geophysical Union, Washington, D.C. 21-31

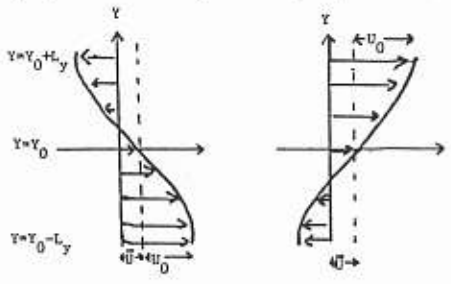

Fig. 1. Basic flow in subtropics
Left: SH. Right NH

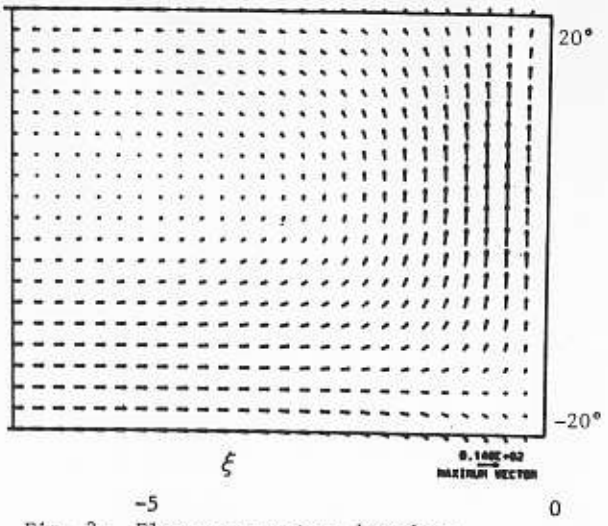

Fig. 2. Flow near eastern boundary.

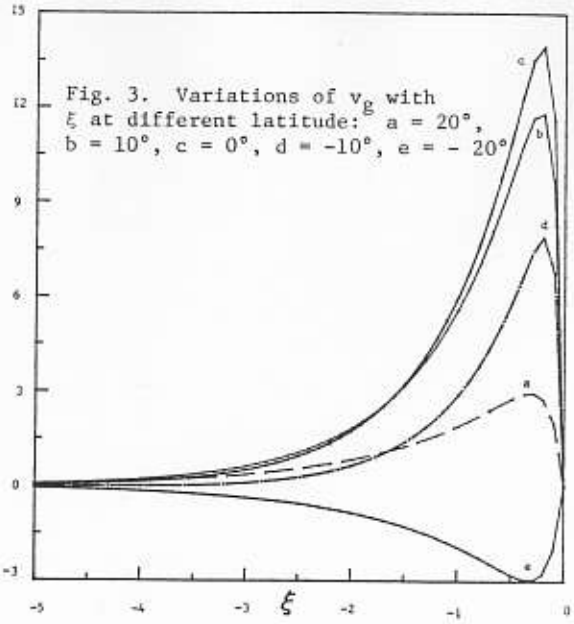

Fig. 3. Variations of v_g with ξ at different latitude: a = 20°, b = 10°, c = 0°, d = -10°, e = - 20°

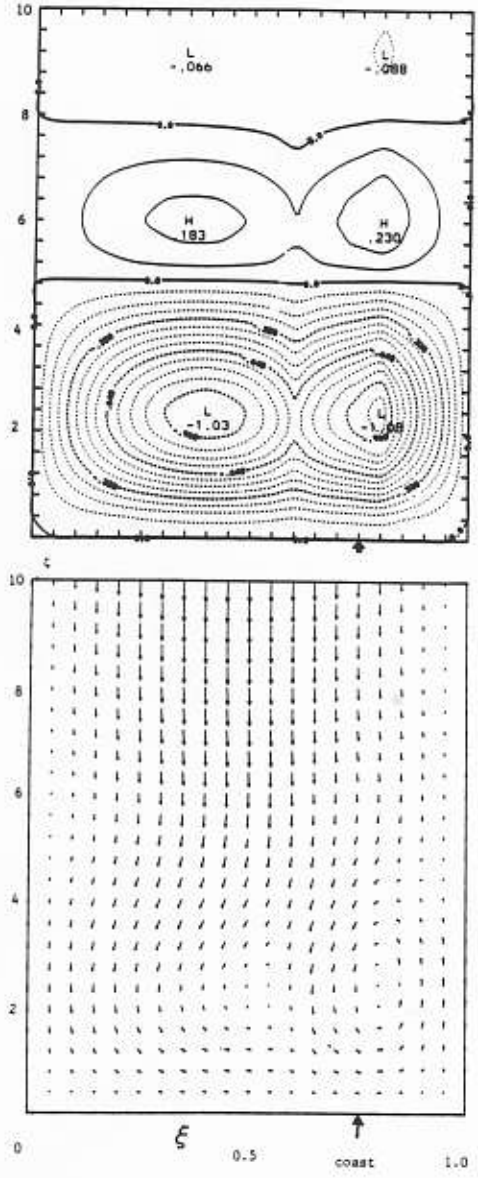

Fig. 4. a. Stream function. b. Total vector velocity in xz-plane.

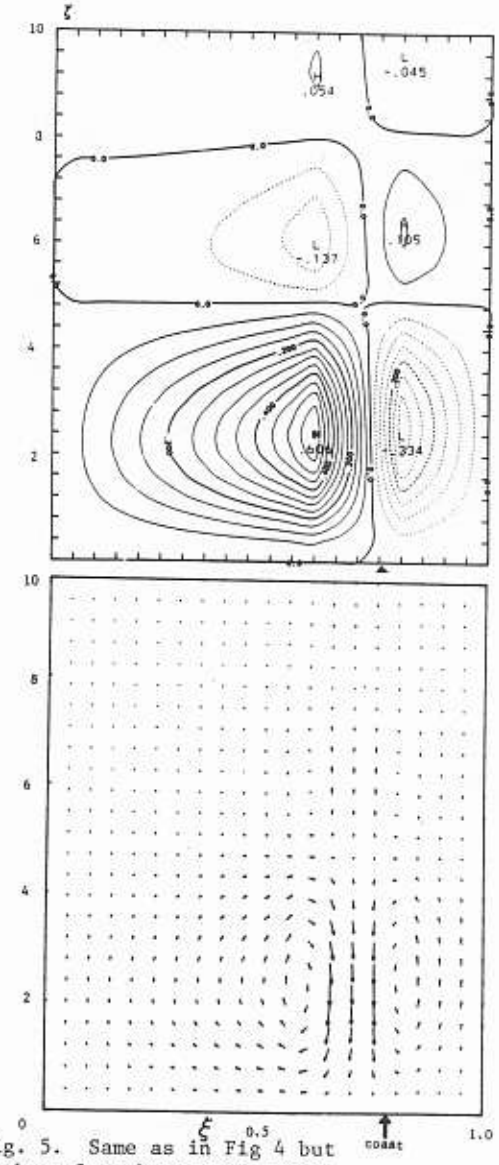

Fig. 5. Same as in Fig 4 but without longshore wind effect.